Supplementary Information

Temporally-regulated quick activation and inactivation of Ras is important for olfactory behaviour

Takayuki Uozumi, Takaaki Hirotsu, Kazushi Yoshida, Ryuji Yamada, Akiya Suzuki, Gun Taniguchi, Yuichi Iino, Takeshi Ishihara

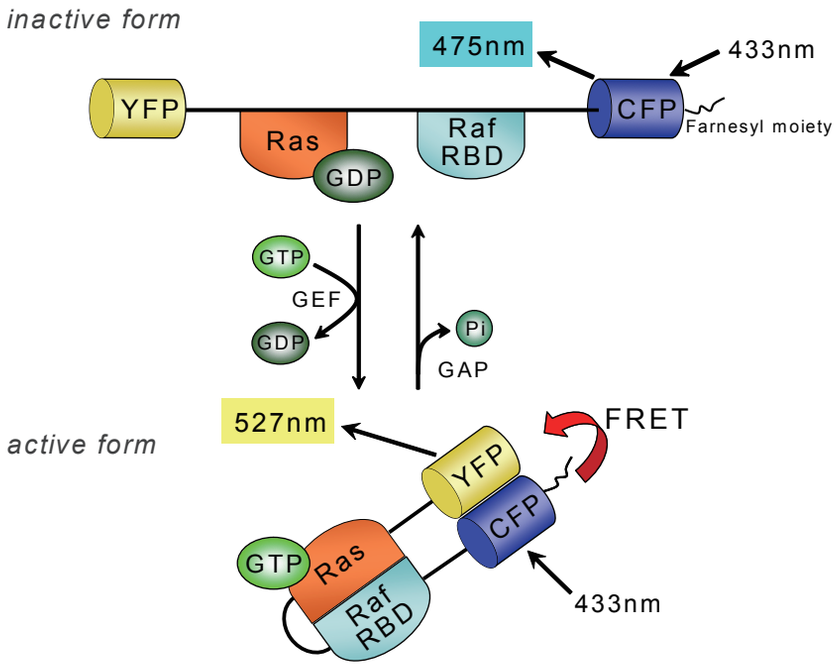

Supplementary Figure 1　Schematic representation of Raichu-Ras.

Raichu-Ras consists of Ras and the Ras-binding domain of Raf (Raf RBD) flanked by YFP and CFP. When Ras is inactivated, Raichu-Ras emits CFP-derived fluorescence at 475 nm in response to an excitation wavelength of 433 nm. On the other hand, when Ras is activated, the conformation of Raichu-Ras changes, FRET (Förster resonance energy transfer) occurs between CFP and YFP, and Raichu-Ras emits YFP-derived fluorescence at 527 nm in response to an excitation wavelength of 433 nm.

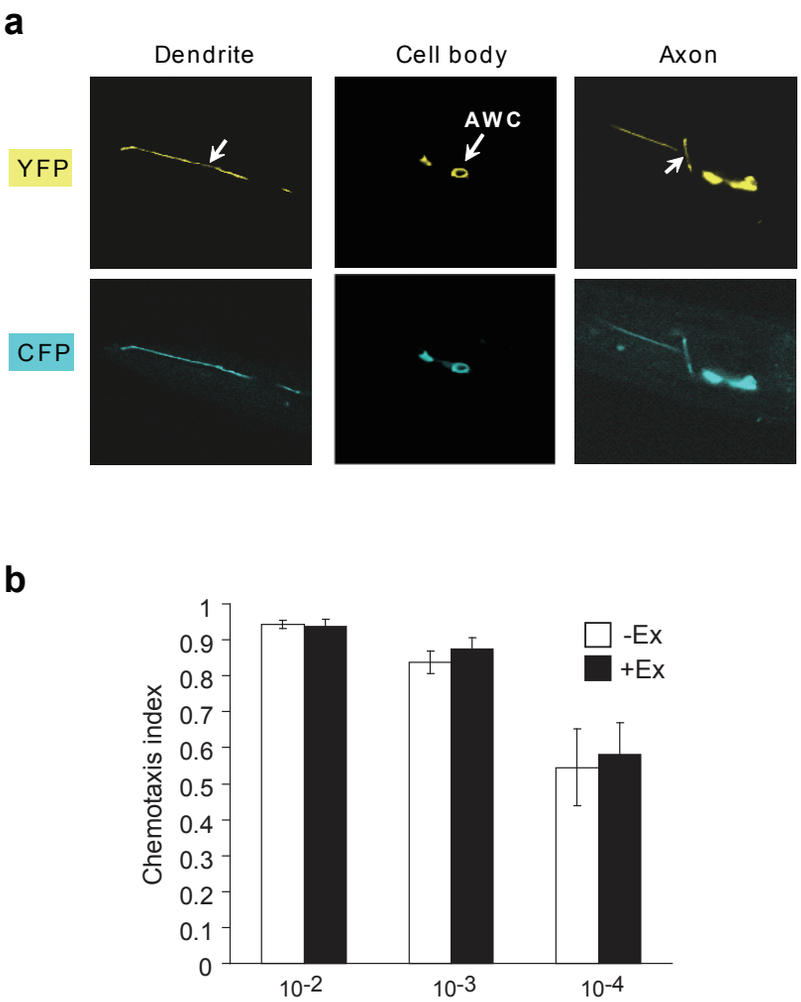

Supplementary Figure 2 Expression of Raichu-Ras in AWC neurons.

(**a**) In AWC neurons of the *odr-1p*::Raichu-Ras strain, YFP and CFP were observed near the membrane regions of dendrites, cell bodies, and axons. (**b**) Chemotaxis in response to isoamyl alcohol in the Ex[*odr-1p*::Raichu-Ras] strain. Worms carrying the transgene (+Ex) and worms not carrying the transgene (−Ex) were compared. Dilutions of isoamyl alcohol are indicated at the bottom of the graph. Error bars indicate SEM. Expression of Raichu-Ras in AWC neurons did not cause a significant reduction in the chemotactic effects of isoamyl alcohol ($P > 0.05$; Student's t test).

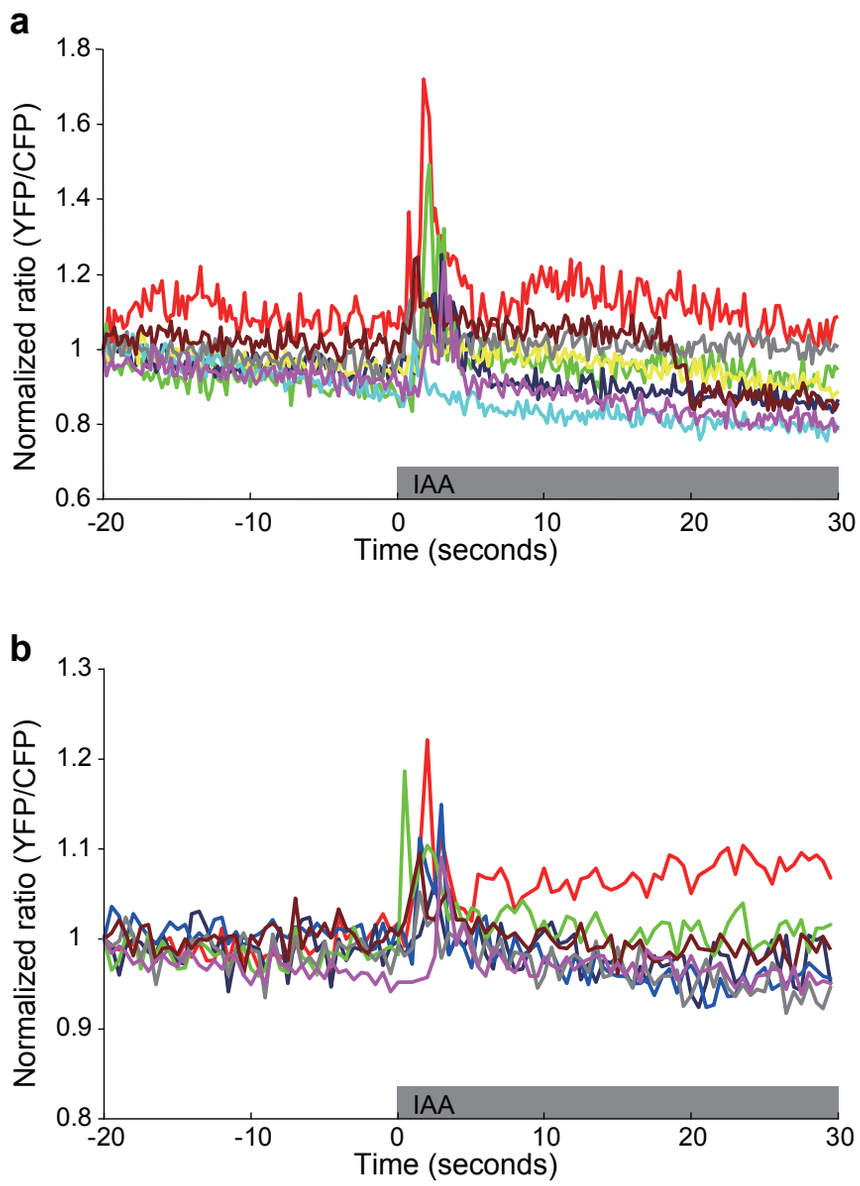

Supplementary Figure 3 Superimposed Ras responses in AWC neurons.

(**a,b**) Changes in the fluorescence ratio from Raichu-Ras after stimulation of AWC neurons with isoamyl alcohol (IAA; final concentration, 5×10^{-4}). Responses were obtained at high time resolution (exposure time, 200 msec; n = 8) using a sensitive ORCA-D2 digital camera (**a**) and at low time resolution (exposure time, 500 msec; n = 7) using a 3CCD digital camera (**b**).

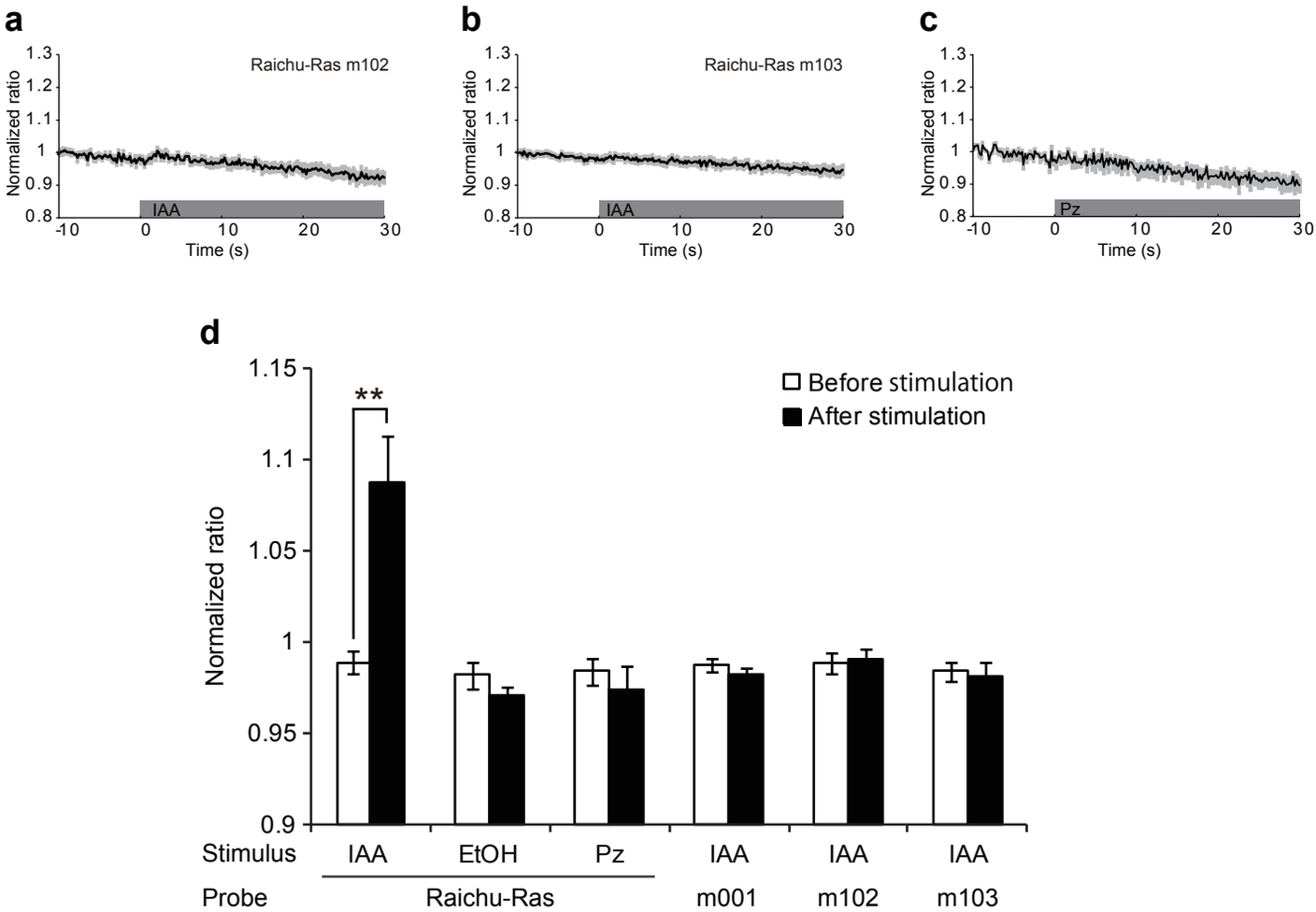

Supplementary Figure 4 Observation of Ras activity in control conditions.

(**a**,**b**) Average ratio (YFP/CFP) from the mutant types of Raichu-Ras (**a**; Raichu-Ras m102, n = 9, **b**; Raichu-Ras m103, n = 13) after application of isoamyl alcohol (IAA). The shaded region around the plotted data represents SEM and gray bar represents existence of odorants. (**c**) Average ratio from the Raichu-Ras after application of pyrazine (Pz) (n = 6). (**d**) Average ratio changes of Raichu-Ras and mutant-types of Raichu-Ras (m001, m102 and m103) during the 10 sec before and after odor stimulation. Error bars indicate SEM and the asterisk indicates a significant difference compared with before stimulation ($P < 0.01$; Student' s t test).

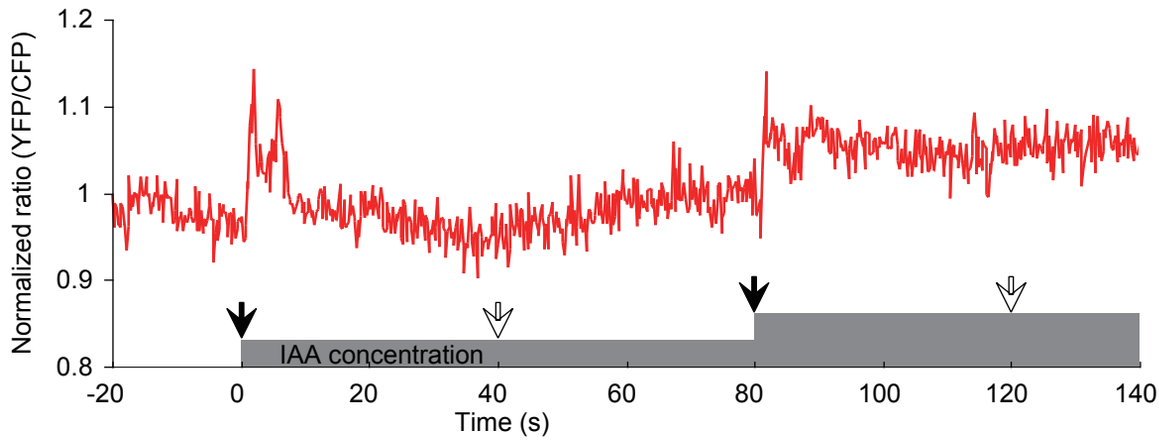

Supplementary Figure 5 Ras activity responds to increase in the odor concentration.

Representative Ras activity in AWC sensory neurons after repeated stimulation with isoamyl alcohol (IAA). Filled arrows represent an increase in the concentration of IAA (the final dilutions of the odorant are 5×10^{-4} and 1×10^{-3} after the first and second stimulation, respectively), whereas open arrows represent sham stimuli that were not associated with an increase in the IAA concentration. Gray bar represent existence of IAA.

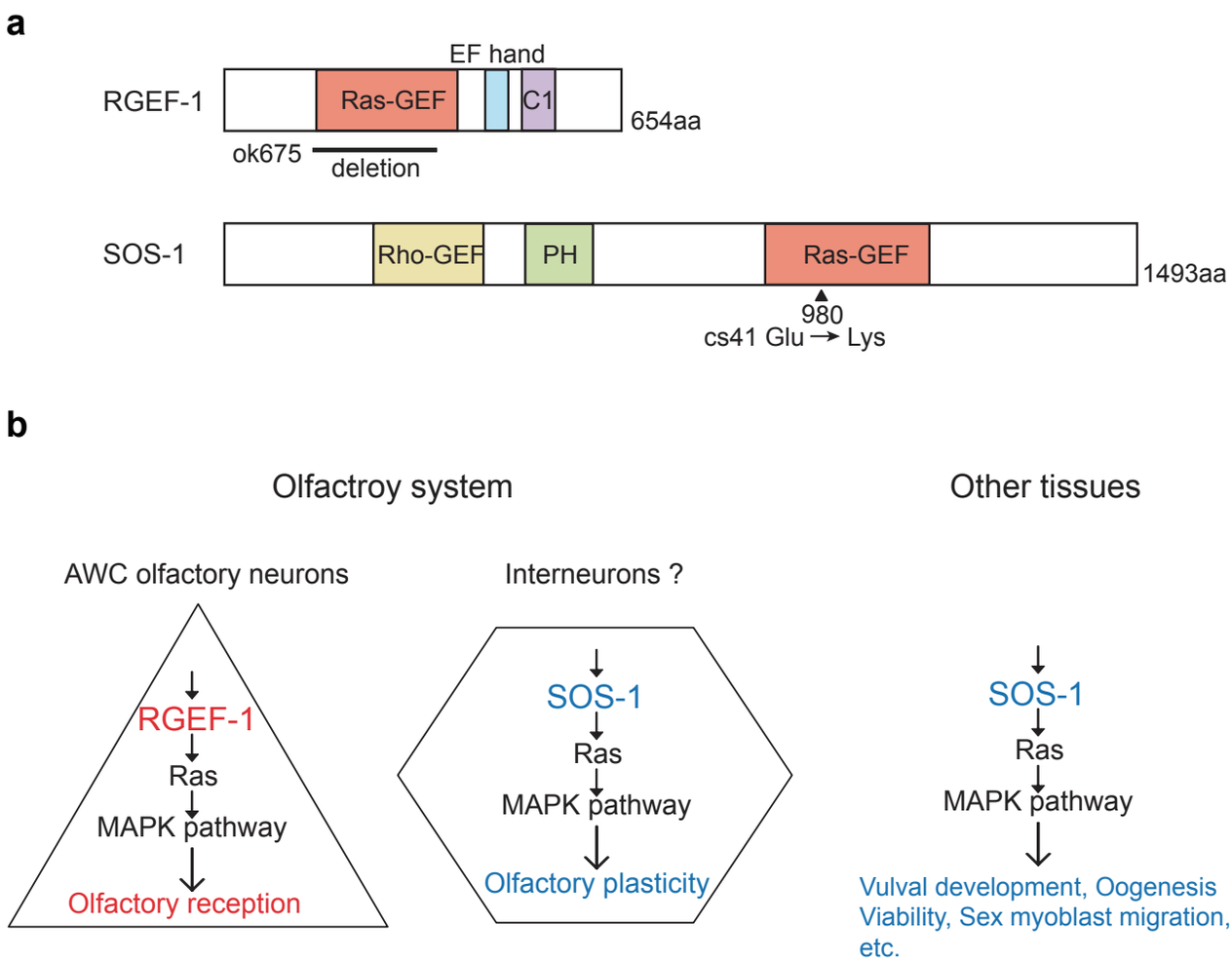

Supplementary Figure 6 Ras-GEFs in the olfactory system and other tissues.

(**a**) Protein motifs in RGEF-1 and SOS-1. RGEF-1 has a Ras-GEF domain, an EF-hand, and a C1 domain. The Ras-GEF domain catalyzes the exchange of GDP for GTP. The EF-hand binds Ca^{2+}. The C1 domain functions as a diacylglycerol-binding region. *ok675* lacks most of the Ras-GEF domain. In contrast, SOS-1 contains Rho-GEF, pleckstrin homology (PH), and Ras-GEF domains. *cs41* has a missense mutation that changes a single amino-acid residue. (**b**) Different Ras-GEFs are used in different mechanisms in the olfactory system of *C. elegans*. RGEF-1 and SOS-1 regulate olfactory recepion and olfactory plasticity, respectively. SOS-1 also functions in other tissues and processes—vulval development, oogenesis, viability, and sex myoblast migration, among others.

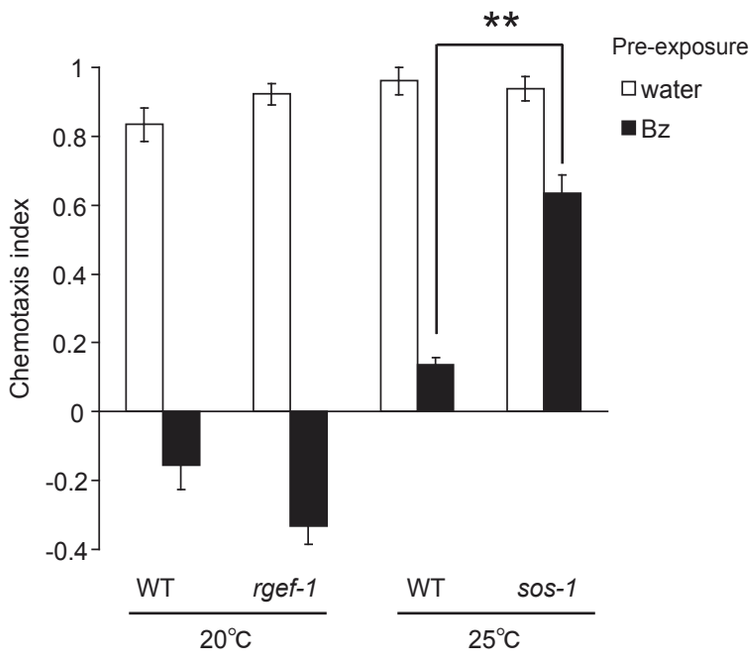

Supplementary Figure 7 Olfactory plasticity phenotypes of Ras-GEF mutants.

After pre-exposure to a 10^{-4} dilution of benzaldehyde (Bz), wild-type animals showed decreased chemotactic responses to a 10^{-2} dilution of benzaldehyde. Open bars represent chemotaxis after exposure to water and filled bars represent chemotaxis after exposure to benzaldehyde. *rgef-1(ok675)* mutants showed normal olfactory plasticity, whereas *sos-1(cs41)*^{ts} mutants displayed defective plasticity after cultivation for 24 hrs at 25°C. Error bars indicate SEM and asterisks indicate significant differences from wild-type values ($P < 0.01$; Student's t test). *rgef-1(ok675)* mutants shows severe defects in naïve chemotaxis to isoamyl alcohol, thus we could not examine isoamly alcohol adaptation.

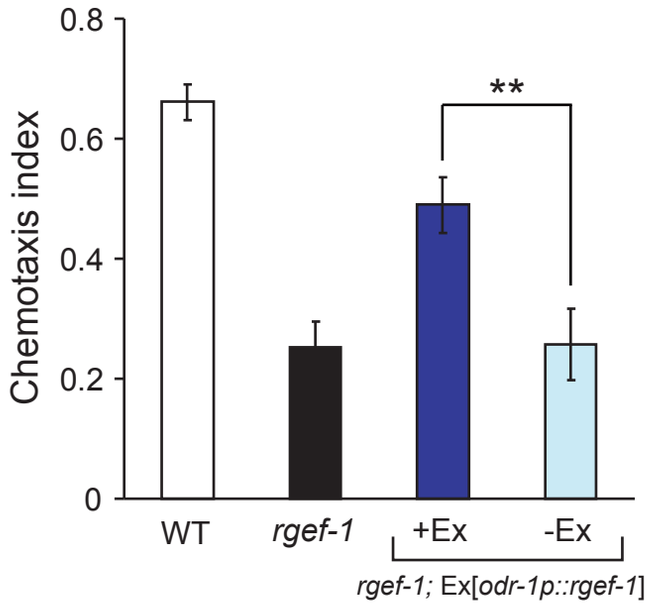

Supplementary Figure 8 RGEF-1 functions in AWC olfactory neurons.

Chemotaxis to isoamyl alcohol (10^{-3} dilution) in wild-type worms (WT), *rgef-1(ok675)* mutants, and *rgef-1*; Ex [*odr-1p::rgef-1*] animals (n ≥ 9 assays). Worms carrying the transgene (+Ex) and worms not carrying the transgene (–Ex) were compared. Error bars indicate SEM and the asterisk indicates a significant difference ($P < 0.01$; Student's t test).

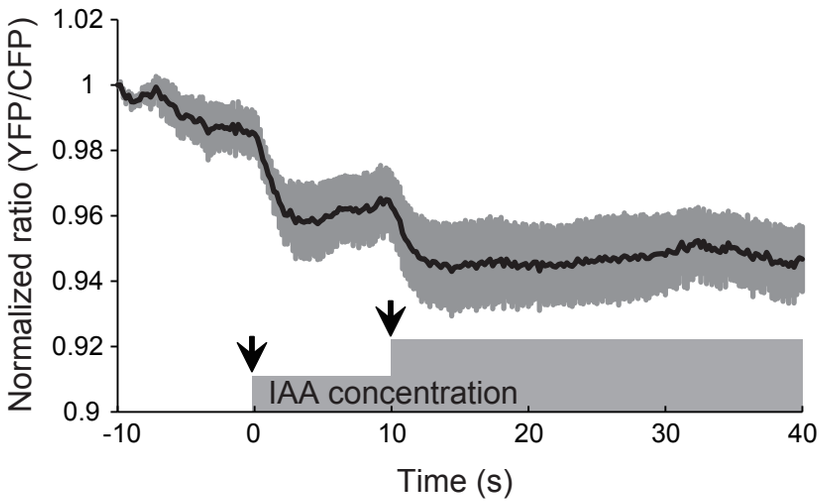

Supplementary Figure 9 Calcium responses of AWC sensory neurons to repeated odour stimuli.
Average ratio (YFP/CFP) changes of yellow cameleon 3.60 in AWC neurons in wild-type animals after repeated addition of isoamyl alcohol stimuli. Filled arrows indicate an increase in the concentration of IAA. Concentrations of IAA used for the first and second stimulation are 1×10^{-7} and 1×10^{-5}, respectively. Light gray shading around the plotted data indicates SEM.

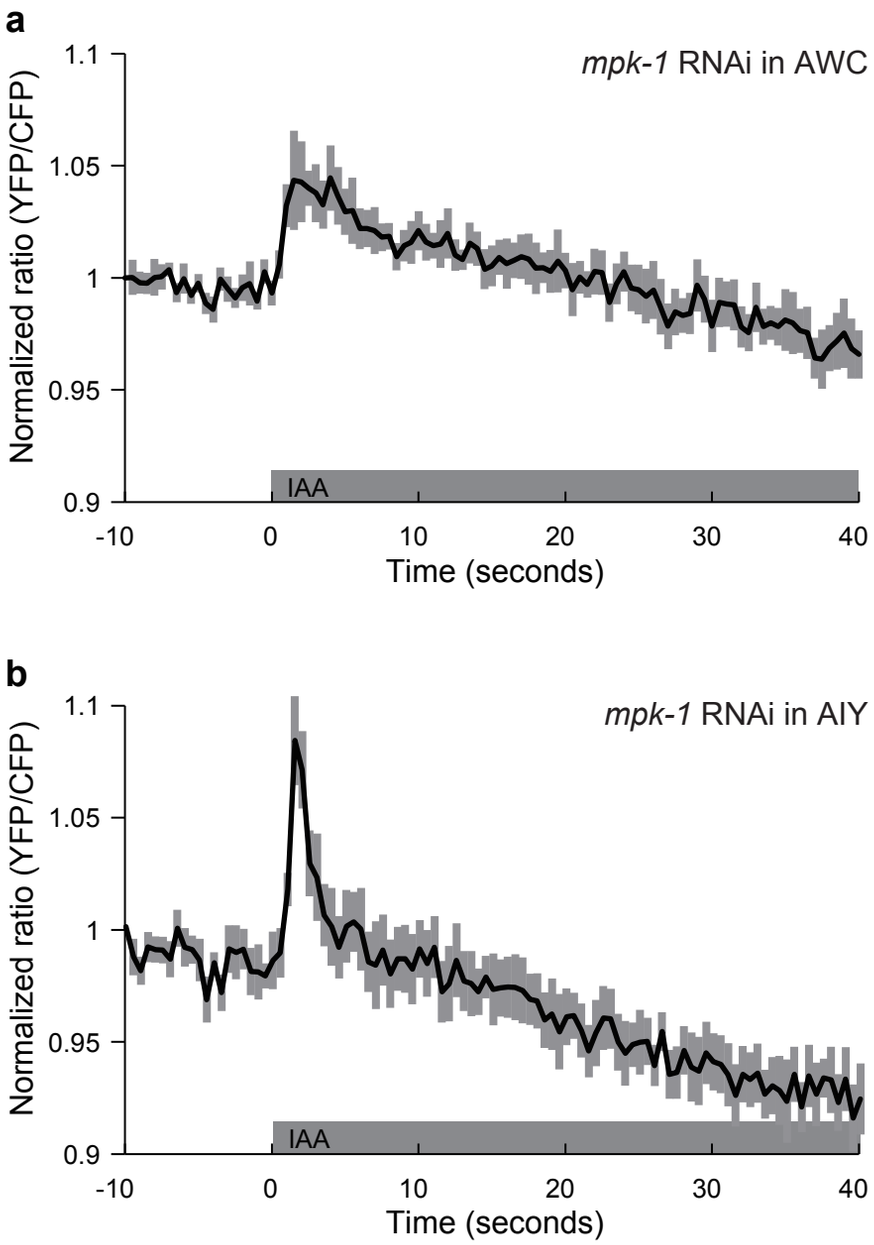

Supplementary Figure 10 Effects of neuron-specific knockdown of *mpk-1* functions on the Ras activity in AWC neurons

Ras activity in AWC neurons in response to 5×10^{-4} dilution of isoamyl alcohol in wild type with knockdown of *mpk-1* functions in AWC (n = 9) (**a**) or AIY (n = 10) (**b**). The shaded region around the plotted data represents SEM.

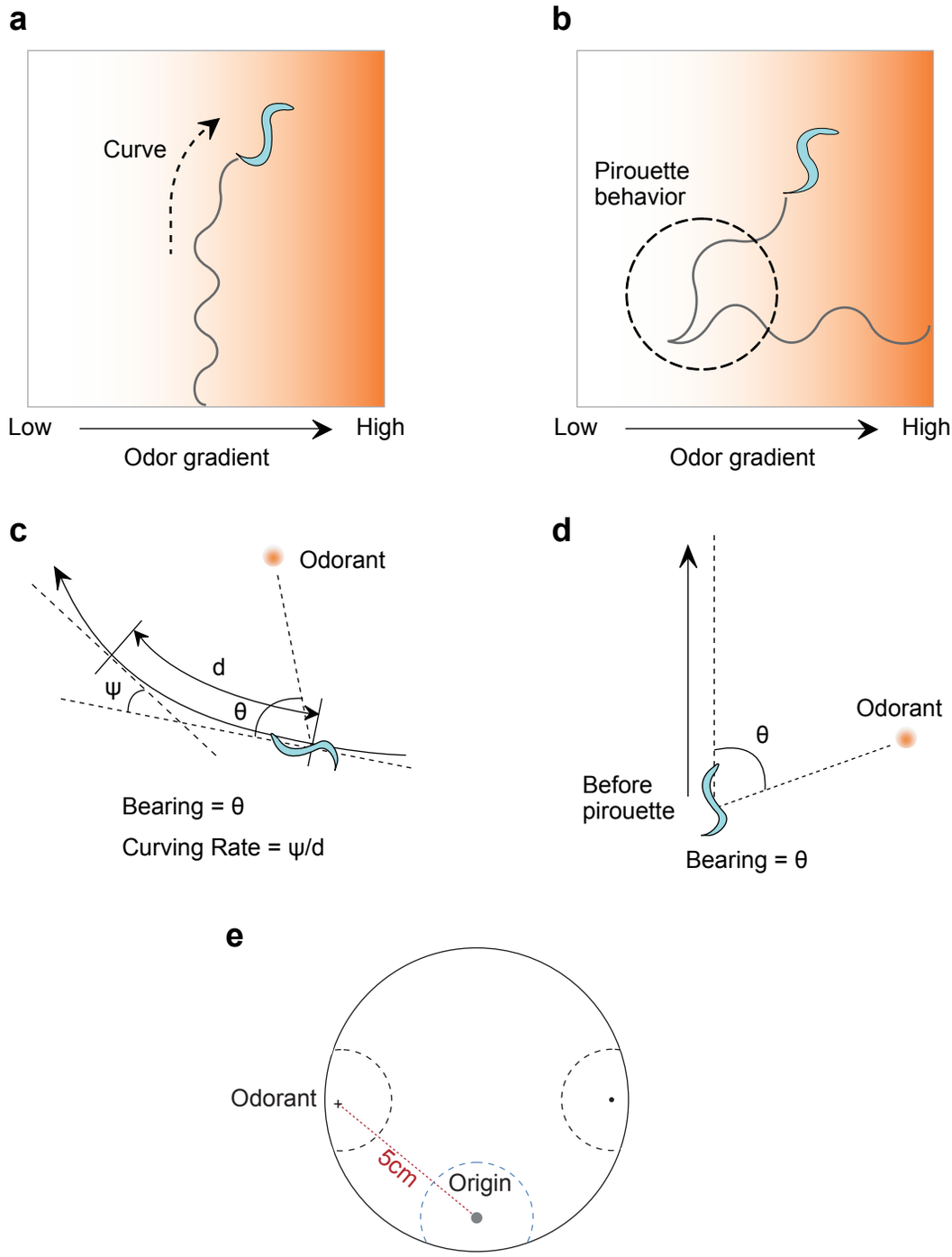

Supplementary Figure 11 Analyses of klinotaxis and klinokinesis

(**a,b**) Schematic representations of klinotaxis (weathervane mechanism) (**a**) and klinokinesis (pirouette mechanism) (**b**). Orange shading indicates the concentration gradient of an odor. (**c,d**) Analyses of klinotaxis (**c**) and klinokinesis (**d**). Bearing (θ)was defined as the angle between the direction to the odor source and the direction oflocomotion. The curving rate (ψ/d) was defined as the change in the direction of locomotion per unit length of advancement. (**e**) The plate design used in this study.

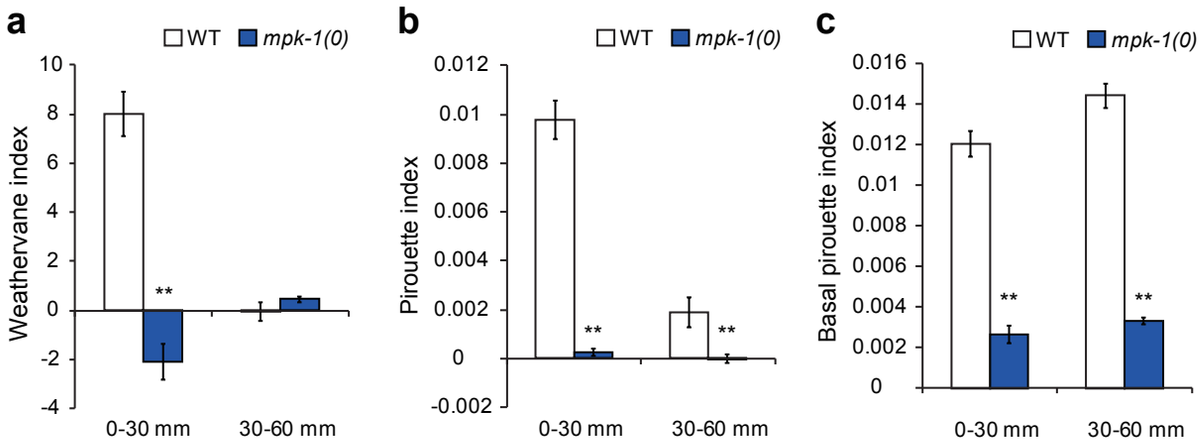

Supplementary Figure 12 Klinotaxis and klinokinesis in the *mpk-1(ga117null)* mutants

Klinotaxis (**a**), klinokinesis (**b**), and the basal pirouette index (**c**) in wild type (WT) (n = 8) and the *mpk-1(ga117)* mutants (n = 8) during chemotaxis to isoamyl alcohol at a dilution of 10^{-4}. Error bars represent SEM. Significant differences compared with wild-type animals are indicated (**$P < 0.01$; Student' s t test). Severe defects in klinokinesis in the *mpk-1* mutants might reflect the large abnormality in the basal pirouette frequency under odour-free conditions.

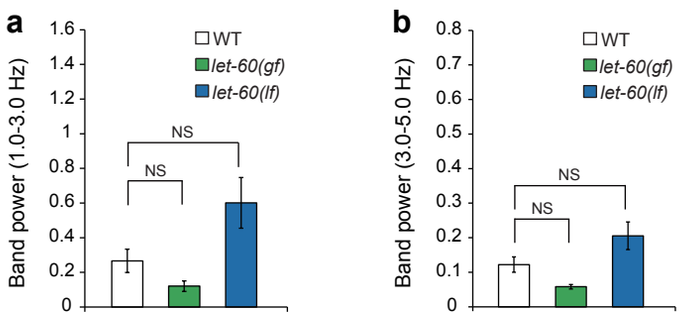

Supplementary Figure 13 Fourier power analysis of AIB calcium responses

(**a**, **b**) The average power of the band (**a**; 1.0-3.0 Hz, **b**; 3.0-5.0 Hz) in wild-type animals (n = 9), *let-60(n1046gf)* mutants (n = 11) and *let-60(n2021lf)* mutants (n = 12). Error bars indicate SEM. There were not significant differences (NS) between wild type and the *let-60* mutants ($P > 0.05$; Dunnett' s test).

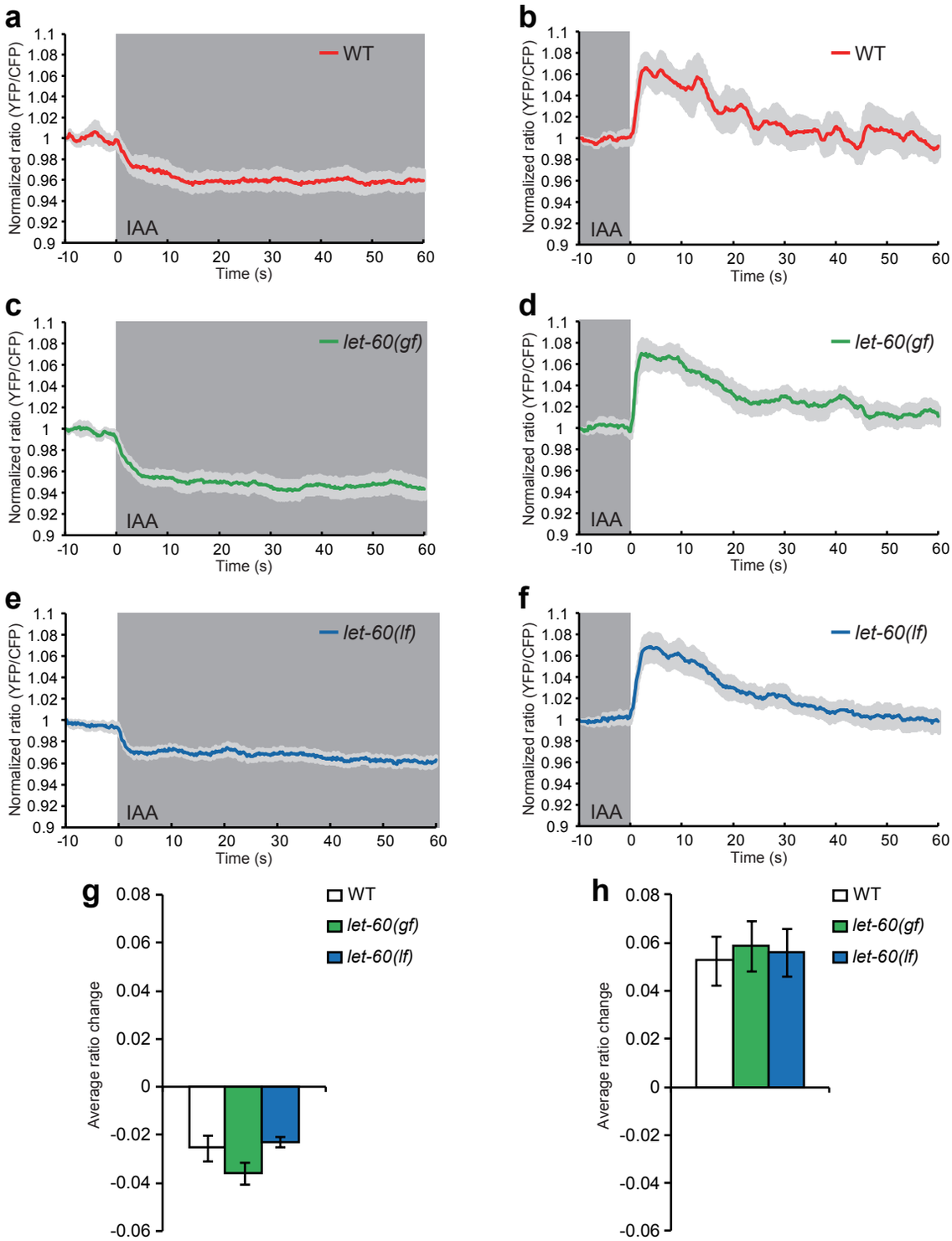

Supplementary Figure 14 Ras signaling does not affect AWC calcium responses.

(**a**-**f**) Average ratio (YFP/CFP) change of yellow cameleon 3.60 in AWC neurons in wild-type animals (**a**,**b**), *let-60 (n1046gf)* mutants (**c**,**d**) and *let-60(n2021lf)* mutants (**e**,**f**) (n=7-13). In all imaging figures, 10^{-4} dilutions of isoamyl alcohol (IAA) were used. Light gray shading around the plotted data indicates SEM and deep gray region indicates existence of IAA. (**g**,**h**) Average ratio changes of YC3.60 in wild type, *let-60(gf)* and *let-60(lf)* mutants during the 10sec before and after odor stimulation. Average ratio change was calculated as (average normalized ratio value during10 sec after odor stimulation) – (average normalized ratio value during 10 sec before odor stimulation). Error bars indicate SEM. There were not significant differences between wild type and the *let-60* mutants ($P > 0.05$; Dunnett' s test).

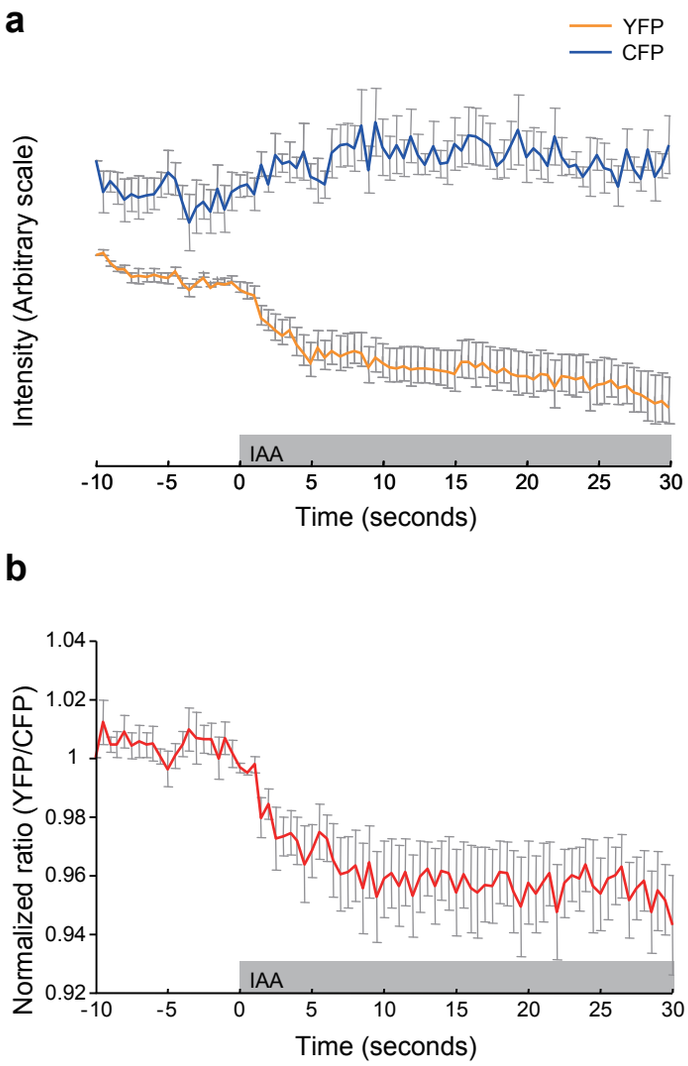

Supplementary Figure 15 Calcium imaging in AWC olfactory neurons.

(**a,b**) Temporal changes of YFP- and CFP-derived fluorescence intensities (**a**) and the fluorescence ratio (**b**) were obtained using yellow cameleon (YC) 3.60 and isoamyl alcohol (IAA) (n = 5). A decrease in the ratio was observed after IAA administration, indicating that the animals sensed the odor stimuli in this system (see Methods). Error bars represent SEM. IAA stimuli were applied at 0 seconds and grey bars denote when IAA was present.

Supplementary Movie 1 Fluorescence change of Raichu-Ras after odor stimulation in AWC neuron.

A movie of fluorescence changes of Raichu-Ras after odour stimulation in an AWC cell body. Isoamyl alcohol stimulus was added at 5 sec. Images are colour-coded with blue indicating low fluorescence ratios, and red indicating high fluorescence ratios and Ras activation. The movie replays at the original speed.